Supramolecular Chemistry
Publication details, including instructions for authors and subscription information:
http://www.informaworld.com/smpp/title~content=t713649759

Metal-organic Coordination Polymers Assembled from Divalent Transition Salts with a Flexible Spacer Ligand: Hydrothermal Syntheses, Crystal Structures, and Luminescent and Magnetic Properties

Yu-Ting Wang[ab]; Xiao-Qing Shen[c]; Yao-Ting Fan[a]; Hong-Chang Yao[a]; Hong-Wei Hou[a]
[a] Department of Chemistry, Zhengzhou University, Henan, P. R. China [b] Department of Chemistry, Henan Institute of Education, Henan, P. R. China [c] School of Materials Science and Engineering, Zhengzhou University, Henan, P. R. China

To cite this Article Wang, Yu-Ting , Shen, Xiao-Qing , Fan, Yao-Ting , Yao, Hong-Chang and Hou, Hong-Wei(2008) 'Metal-organic Coordination Polymers Assembled from Divalent Transition Salts with a Flexible Spacer Ligand: Hydrothermal Syntheses, Crystal Structures, and Luminescent and Magnetic Properties', Supramolecular Chemistry, 20: 5, 501 — 515
To link to this Article: DOI: 10.1080/10610270701457962
URL: http://dx.doi.org/10.1080/10610270701457962

Supramolecular Chemistry, July–August 2008 Vol. 20 (5), pp. 501–515

Metal–organic Coordination Polymers Assembled from Divalent Transition Salts with a Flexible Spacer Ligand: Hydrothermal Syntheses, Crystal Structures, and Luminescent and Magnetic Properties

YU-TING WANG[a,b], XIAO-QING SHEN[c], YAO-TING FAN[a,*], HONG-CHANG YAO[a] and HONG-WEI HOU[a,*]

[a]*Department of Chemistry, Zhengzhou University, Henan 450052, P. R. China;* [b]*Department of Chemistry, Henan Institute of Education, Henan 450014, P. R. China;* [c]*School of Materials Science and Engineering, Zhengzhou University, Henan 450052, P. R. China*

(Received 20 March 2007; Accepted 16 May 2007)

Seven new metal-organic coordination polymers, $[M(tzda)(H_2O)_4]_n$ [M = Co(1), Ni (2) and Zn(3)], $[Zn(tzda)(4,4'\text{-bipy})]_n$ (4), $[Cd(tzda)(4,4'\text{-bipy})_{0.5}(H_2O)]_n$ (5) and $[M(tzda)(4,4'\text{-bipy})(H_2O)]_n$ [M = Co(6), Ni(7)] [H_2tzda = (1,3,4-thiadiazole-2,5-diyldithio)diacetic acid, 4,4′-bipy = 4,4′-bipyridine] have been hydrothermally synthesized and structurally characterized by X-ray single crystal diffraction. Compounds 1–3 display similar 1D zigzag chain structure. Compound 4 possesses a 2D-layered architecture generated from $[Zn(tzda)]_n$ moiety with double-chain structure cross-linking 4,4′-bipy spacers, while compound 5 consists of —Cd—O-CO—Cd—OCO— chains cross-linked through $-CH_2SC_2N_2SSCH_2-$ spacers of tzda anions and 4,4′-bipy, also showing a 2D-layered structure. The structures of 6 and 7 seem more complicated, in which the $[M(tzda)]_n$ layered subunits are extended to unique 3D framework by the bridging 4,4′-bipy ligand. Photoluminescence investigations reveal that 4 and 5 both display strong blue emissions in the solid state at room temperature, which could be significant in the field of luminescent materials. The magnetic studies of 6 and 7 show both display the characteristics of a weak antiferromagnetic coupling between metal ions in the system mediated by carboxylate bridges.

Keywords: Flexible carboxylate ligands; Coordination polymers; Hydrothermal synthesis; Luminescent property; Magnetic property

INTRODUCTION

In recent years, the synthesis and characterization of metal-organic coordination polymers based on polycarboxylate ligands have been of great interest because of their fascinating architectures and topologies as well as their unexpected properties for potential applications in molecular recognition, magnetism, catalysis, optoelectronic devices, and so on [1–11]. Great efforts have been focused on rigid aromatic ligands, such as 1,4-benzenedicarboxylate [12,13], 1,3,5-benzenetricarboxylate [14–16], 4,4′-biphenyldicarboxylic acid [17], and 2,2′-bipyridyl-4,4′-carboxylic acid [18]. Coordination polymers assembled by metal salts with flexible carboxylate-containing ligands are not well done to now, possibly due to the difficulties in predicting the resulted framework structures [19,20]. However, in contrast to the rigid ligands, the flexible ones may exhibit more conformational and coordination versatility. Thus they can meet the coordination geometrical requirement of metal ions through changing their conformation and coordination modes and hence can control and adjust the structure of the resulting coordination frameworks [21]. So far, most reported flexible carboxylate-containing ligands are aliphatic [22,23]. Examples of flexible carboxylate-containing ligands containing aromatic feature are far less common [24,25].

Against the above backgrounds, we focused our attention on the synthesis, structure, and property of coordination frameworks with a flexible dicarboxylate ligand H_2tzda [H_2tzda = (1,3,4-thiadiazole-2,5-diyldithio)diacetic acid, which remain almost unexplored in the field of crystal engineering and supramolecular chemistry [26–29]. The two

*Corresponding authors. Tel/fax: +86(0) 371 67766017 (Y.-T. Fan). E-mail: yt.fan@zzu.edu.cn or ytfan1207@yahoo.com.cn

ISSN 1061-0278 print/ISSN 1029-0478 online © 2008 Taylor & Francis
DOI: 10.1080/10610270701457962

$-SCH_2-$ groups make it more flexible than those rigid aromatic carboxylic acids, whilst the existence of thiadiazole ring endows it with aromatic feature. And the existence of sulphur atom can also make it possible to form S···S weak interactions that play an important role in the supramolecular compounds. Recent studies on the rare earth coordination polymers of H_2tzda in our lab have confirmed that H_2tzda is a good building block because of its various conformation and coordination modes [29]. The successful syntheses of these complexes prompted us to carry out the assembly of transition metal salts with H_2tzda to build new coordination polymers. In order to construct high-dimensional structures, we also tried to introduce a second bridging ligand 4,4′-bipy into the reaction system since the combination of both polycarboxylate and rigid linear connector 4,4′-bipy or analogues helps to assemble high-dimensional supramolecular networks [30–32]. Herein we report the hydrothermal syntheses and characterizations of seven new transition metal coordination polymers with H_2tzda: $[M(tzda)(H_2O)_4]_n$ [M = Co (**1**), Ni (**2**) and Zn (**3**)], $[Zn(tzda)(4,4'\text{-bipy})]_n$ (**4**), $[Cd(tzda)(4,4'\text{-bipy})_{0.5}(H_2O)]_n$ (**5**) and $[M(tzda)(4,4'\text{-bipy})(H_2O)]_n$ [M = Co (**6**), Ni (**7**)]. Fortunately, among them, a rare structural feature with 'the Great Wall' shape of China is observed in the polymers **6** and **7**. In addition, the properties of these polymers, such as photoluminescent and magnetic behaviors, are also investigated.

EXPERIMENTAL SECTION

Materials and Measurements

All starting chemicals were of reagent grade and used without further purification. Elemental analyses (C, H, N) were performed on a Carlo-Erba 1160 Elemental Analyzer. IR spectra were recorded in the region of 4000–400 cm^{-1} on a Nicolet NEXUS 470-FTIR Spectrophotometer with pressed KBr pellets. ^{1}H NMR spectra were determined at room temperature on Bruker DPX 400 Spectrometer. Themogravimetric analyses were carried out with a NETZSCH STA 409 unit at a heating rate of 10°C/min under a nitrogen atmosphere. Excitation and emission spectra were obtained on a F-4500 HITACHI Fluorescence Spectrophotometer. Variable-temperature magnetic susceptibility data were obtained on a SQUID Susceptometer (Quantum Design, MPMS-5) in the temperature range of 5.0–300 K with an applied field of 500G. The diamagnetic contributions of the samples were corrected by using Pascal's constants [33].

(1,3,4-thiadiazole-2,5-diyldithio)diacetic acid (H_2tzda) was prepared according to the literature method [28]. Elemental Anal. Calcd (%) for $C_6H_6N_2O_4S_3$: C, 27.07; H, 2.26; N, 10.53. Found: C, 27.12; H, 2.18; N, 10.19. IR data (cm^{-1}): 3082(m), 2983(m), 2927(m), 1735(s), 1712(s), 1384(s), 1364(m), 1299(m), 1202(s), 1182(s), 1050(s), 893(m), 780(m), 649(w). ^{1}H NMR (300 MHz, DMSO, 25°C): $\delta = 13.0479$ (s, 2H, COOH), 4.1414(s, 4H, CH_2).

Synthesis of $[M(tzda)(H_2O)_4]_n$ [M = Co(1), Ni(2), Zn(3)]

A mixture of $M(NO_3)_2{\cdot}6H_2O$ (1 mmol, M = Co, 291 mg; M = Ni, 291 mg; M = Zn, 297 mg), H_2tzda (1 mmol, 266 mg), NaOH (2 mmol, 80 mg) and deionized water (15 ml) was sealed in a Teflon-lined stainless steel vessel (25 ml), and then heated at 120°C for 4 days (**1** and **2**) or 6 days (**3**). After cooled to room temperature, crystals of **1** (red, prismatic), **2** (green, prismatic), and **3** (colorless, prismatic) were collected by filtration, respectively. Yield: 29% (**1**), 34% (**2**) and 26% (**3**) (based on transition metal). Anal. Calcd (%) for **1** ($C_6H_{12}CoN_2O_8S_3$): C, 18.21; H, 3.04; N, 7.08. Found: C, 18.11; H, 3.21; N, 6.99. Anal. Calcd (%) for **2** ($C_6H_{12}NiN_2O_8S_3$): C, 18.22; H, 3.04; N, 7.09. Found: C, 18.19; H, 3.15; N, 7.01. Anal. Calcd (%) for **3** ($C_6H_{12}ZnN_2O_8S_3$): C, 17.92; H, 2.99; N, 6.97. Found: C, 17.88; H, 3.04; N, 7.01. IR data (KBr, cm^{-1}) for **1**: 3273(s), 1602(s), 1387(s), 1238(s), 1176(w), 1066(m), 867(w), 780(m), 683(m); for **2**: 3247(s), 1599(s), 1388(s), 1239(s), 1172(w), 1066(m), 889(w), 778(m), 686(m); for **3**: 3257(s), 1601(s), 1392(s), 1238(s), 1173(w), 1068(m), 879(w), 778(m), 684(m).

Synthesis of $[Zn(tzda)(4,4'\text{-bipy})]_n$ (4)

A mixture of $Zn(NO_3)_2{\cdot}6H_2O$ (0.4 mmol, 119 mg), H_2tzda (0.4 mmol, 106 mg), NaOH (0.8 mmol, 32 mg), 4,4′-bipy (0.4 mmol, 62 mg) and deionized water (15 ml) was sealed in a Teflon-lined stainless steel vessel (25 ml), and then heated at 120°C for 7 days. After cooled to room temperature, colorless block crystals of **4** were collected by filtration. Yield: 39% based on Zn. Anal. Calcd (%) for $C_{16}H_{12}ZnN_4O_4S_3$: C, 39.52; H, 2.47; N, 11.53. Found: C, 39.33; H, 2.61; N, 11.21 IR data (KBr, cm^{-1}): 1603(s), 1589(s), 1413(s), 1393(s), 1222(s), 1174(m), 1072(s), 1048(s), 929(m), 895(m), 823(s), 774(s), 679(m), 634(m).

Syntheses of $[Cd(tzda)(4,4'\text{-bipy})_{0.5}(H_2O)]_n$ (5) and $[M(tzda)(4,4'\text{-bipy})(H_2O)]_n$ [M = Co(6), Ni(7)]

A mixture of $Cd(NO_3)_2{\cdot}4H_2O$ (0.4 mmol, 123 mg) or $M(NO_3)_2{\cdot}6H_2O$ (M = Co, 0.4 mmol, 116 mg; M = Ni, 0.4 mmol, 116 mg), H_2tzda (0.4 mmol, 106 mg), NaOH (0.8 mmol, 32 mg), 4,4′-bipy (0.2 mmol, 31 mg,) and deionized water (15 ml) was sealed in a Teflon-lined stainless steel vessel (25 ml), and then heated at 120°C for 4 days. After cooled

to room temperature, crystals of **5** (colorless, needle-like), **6** (red, block-like) and **7** (green, block-like) were collected by filtration, respectively. Yield: 17% (**5**), 24% (**6**) and 20% (**7**) (based on transition metal). Anal. Calcd (%) for **5** ($C_{11}H_{10}CdN_3O_5S_3$): C, 27.92; H, 2.12; N, 8.88. Found: C, 27.79; H, 2.27; N, 8.64. Anal. Calcd (%) for **6** ($C_{16}H_{14}CoN_4O_5S_3$): C, 38.60; H, 2.81; N, 11.26. Found: C, 38.54; H, 2.91; N, 11.19. Anal. Calcd (%) for **7** ($C_{16}H_{14}NiN_4O_5S_3$): C, 38.62; H, 2.82; N, 11.26. Found: C, 38.50; H, 2.96; N, 11.15. IR data (KBr, cm^{-1}) for **5**: 3499(s), 1582(s), 1412(s), 1389(s), 1220(s), 1180(w), 1068(m), 1050(m), 940(m), 897(m), 814(s), 789(w), 686(m), 629(w); for **6**: 3504(s), 1608(s), 1577(s), 1403(s), 1381(s), 1218(m), 1167(w), 1065(m), 1053(m), 927(w), 876(w), 820(s), 693(w), 635(m); for **7**: 3507(s), 1609(s), 1570(s), 1407(s), 1383(s), 1217(m), 1189(w), 1066(m), 1048(m), 924(w), 876(w), 821(s), 699(w), 638(m).

X-ray Crystallographic Studies

Single crystals of **1** (0.20 × 0.16 × 0.16 mm), of **2** (0.20 × 0.18 × 0.16 mm), of **3** (0.30 × 0.23 × 0.17 mm), of **4** (0.26 × 0.22 × 0.14 mm), of **5** (0.35 × 0.19 × 0.13 mm), of **6** (0.32 × 0.19 × 0.17 mm), and of **7** (0.50 × 0.26 × 0.16 mm) were selected for indexing and intensity data collection. The intensity data for **1**–**3** were collected at 291(2)–293(2) K on a Rigaku RAXIS-IV image plate area detector with graphite-monochromatized Mo-*K*α ($\lambda = 0.71073$ Å) while the intensity data for **4**–**7** were collected at 291(2)–294(2) K on a Bruker Smart CCD diffractometer equipped with graphite-monochromatized Mo-*K*α ($\lambda = 0.71073$ Å).

All of the structures were solved by direct methods and expanded using Fourier techniques. The non-hydrogen atoms were refined with anisotropic thermal parameters. Hydrogen atoms were located at calculated positions and refined isotropically. The final cycle of full-matrix least squares refinement was based on the observed reflections and variable parameters. Friedel pairs for compounds **1**–**3** were not merged in the refinements. While the carbon-bound H atoms were placed at calculated positions and refined as riding, the oxygen-bound H atoms were located in different maps and refined with fixed Uiso. All calculations were performed using the SHELXL crystallographic software package [34]. Crystallographic data and structural refinements are summarized in Tables I and II. Selected bond distances and angles are listed in Table III.

RESULTS AND DISCUSSION

Preparation of Compounds 1–7

Compounds **1**–**7** were prepared as neutral molecular complexes by hydrothermal reactions of ligand H_2tzda or mixed ligands of H_2tzda and 4,4′-bipy with different metal ions under different conditions. They are stable under ambient conditions and insoluble in common organic solvents, being consistent with their polymeric nature.

In fact, in the preparation of **1**–**7**, both the conventional solution method and the hydrothermal method have been adopted. Reaction of H_2tzda and transition metal ions in the presence of NaOH in MeOH/H_2O at room temperature can also afford the 1D zigzag coordination polymeric chains of **1**–**3** ($[M(tzda)(H_2O)_4]_n$ [M = Co(**1**), Ni(**2**), Zn(**3**)]). However, once neutral rigid ligand 4,4′-bipy was introduced into the solution reaction system as an auxiliary ligand to construct high-dimensional structures, an uncharacterized precipitate insoluble in common solvents was obtained. It is obvious that

TABLE I Crystallographic data and structure refinement parameters for **1**–**3**

Compounds	**1**	**2**	**3**
Empirical formula	$C_6H_{12}Co\ N_2O_8\ S_3$	$C_6H_{12}Ni\ N_2O_8\ S_3$	$C_6H_{12}ZnN_2O_8\ S_3$
Formula weight	395.29	395.07	401.73
Crystal system	Monoclinic	Monoclinic	Monoclinic
Space group	$P2_1$	$P2_1$	$P2_1$
a (Å)	5.2164(10)	5.1717(10)	5.1549(5)
b (Å)	10.129(2)	10.037(2)	9.5031(8)
c (Å)	13.408(3)	13.464(3)	13.6385(13)
α (°)	90	90	90
β (°)	90.57(3)	91.40(3)	94.790(3)
γ (°)	90	90	90
V (Å^3)	708.4(2)	698.7(2)	665.78(11)
Z	2	2	2
μ, mm^{-1}	1.689	1.873	2.353
D_c, g·cm^{-3}	1.853	1.878	2.004
$F(000)$	402	404	408
GOF on F^2	1.040	1.082	1.071
R_1, wR_2 ($I > 2\sigma(I)$)	0.0289, 0.0708	0.0263, 0.0734	0.0482, 0.1144
R_1, wR_2 (all data)	0.0303, 0.0718	0.0279, 0.0744	0.0550, 0.1217
$\Delta\rho_{max}$, $\Delta\rho_{min}$ (e·Å^{-3})	0.461, −0.546	0.250, −0.445	0.545, −0.513

$R_1 = \Sigma||F_0| - |F_c||/\Sigma|F_0|$; $wR_2 = [\Sigma w(F_0^2 - F_c^2)^2/\Sigma w(F_0^2)^2]^{1/2}$.

TABLE II Crystallographic data and structure refinement parameters for **4**–**7**

Compounds	**4**	**5**	**6**	**7**
Empirical formula	$C_{16}H_{12}Zn\ N_4O_4S_3$	$C_{11}H_{10}CdN_3O_5S_3$	$C_{16}H_{14}CoN_4O_5S_3$	$C_{16}H_{14}NiN_4O_5S_3$
Formula weight	485.85	472.80	497.42	497.20
Crystal system	Triclinic	Monoclinic	Orthorhombic	Monoclinic
Space group	$P\bar{1}$	$P2_1/n$	*Pbca*	$P2_1/c$
a (Å)	8.998(2)	12.5419(14)	18.0955(12)	22.5407(19)
b (Å)	10.226(2)	8.4934(10)	9.0501(6)	17.8834(15)
c (Å)	11.376(3)	15.700(2)	22.5878(15)	9.1269(8)
α (°)	64.307(3)	90	90	90
β (°)	77.871(3)	113.374(3)	90	95.905(2)
γ (°)	74.480(4)	90	90	90
V (Å^3)	903.5(4)	1535.2(3)	3699.1(4)	3659.6(5)
Z	2	4	8	8
μ, mm^{-1}	1.739	1.858	1.306	1.443
D_c, g·cm^{-3}	1.786	2.046	1.786	1.805
$F(000)$	492	932	2024	2032
GOF on F^2	1.037	1.041	1.046	1.086
R_1, wR_2 ($I > 2\sigma(I)$)	0.0328, 0.0850	0.0181, 0.0454	0.0247, 0.0620	0.0416, 0.1547
R_1, wR_2 (all data)	0.0393, 0.0900	0.0196, 0.0466	0.0274, 0.0638	0.0464, 0.1582
$\Delta\rho_{max}$, $\Delta\rho_{min}$ (e·Å^{-3})	0.543, −0.687	0.493, −0.455	0.305, −0.366	0.865, −0.549

$R_1 = \Sigma||F_o| - |F_c||/\Sigma|F_o|$; $wR_2 = [\Sigma w(F_o^2 - F_c^2)^2/\Sigma\ w(F_o^2)^2]^{1/2}$.

the hydrothermal reaction should be employed to obtain extended structural motifs because it can not only enhance metal-ligand interactions and produce metastable compounds, which may not be accessible by conventional methods, but also promote crystal growth [35–37]. Thus, the hydrothermal reactions of H_2tzda with 4,4′-bipy and transition metal salts in the presence of NaOH afforded 2D-layered architectures of **4**–**5** and 3D frameworks of **6**–**7**.

Description of the Crystal Structures

Crystal Structure of [M(tzda)(H$_2$O)$_4$]$_n$ [M = Co(1), Ni(2), Zn(3)]

Single-crystal X-ray diffraction analyses reveal that compounds **1**, **2** and **3** crystallize in monoclinic with space group $P2_1$ and display similar one-dimensional zigzag chains consisting of pseudo square-planar $M(H_2O)_4$ [M = Co for **1**, Ni for **2**, and Zn for **3**] bridged tzda ligands, as shown in Fig. 1a. Each metal ion shows a slightly distorted octahedral geometry with four water molecules in the equatorial basal plane and two oxygen atoms from different tzda at the axial positions [O1—Co—O4A = 176.83(17)° for **1**, O1—Ni—O4A = 176.91(18)° for **2**, and O1—Zn—O4A = 174.4(3)° for **3**]. The metal ion is coplanar with four coordinated water molecules and lies in the center of the equatorial plane. The tzda ligand exhibits completely *trans*-configuration and bridges two metal ions in bis-monodentate fashion in **1**–**3**, generating a 1D zigzag chain along *c* axis, in which M···M distances separated by tzda are 13.408 Å in **1**, 13.464 Å in **2**, and 13.639 Å in **3**, respectively.

Significantly, although they have similar cell parameters (Table I) and display similar 1D chain structure, the crystal packing structures of **1**–**3** are not completely uniform due to the formation of different hydrogen-bonding (Table SI, Supplementary Material) and S···S weak interactions based on the flexibility of tzda ligands. In compounds **1**–**3**, all the coordinated water molecules and tzda ligands are involved in forming the H-bonding interactions. In **1**, two types of intrachain hydrogen bonds formed between coordinated water molecules and uncoordinated carboxylate O atom [O7—H7E···O2, O5—H5F···O3a (a: x, y, z + 1)] stabilize the 1D polymeric structure, and another two types of interchain hydrogen bonds formed between the water ligands and coordinated carboxylate O atoms from adjacent chain [O6—H6E···O4b, O8—H8F···O1c (b: x − 1, y, z + 1; c: x + 1, y, z)] result in a 2D-layered supramolecular network in *ac* plane (Fig. 1b). Then these hydrogen-bonded 2D layers are stacked together in the sequence ABAB and connected by other four types of hydrogen bonds, formed by the coordinated water molecules with uncoordinated carboxylate O atoms and thiadiazole N atoms [O5—H5E···O2d, O8—H8E···O2d, O6—H6F···N2e, O7—H7F···N1e (d: −x + 1, y − 1/2, −z + 1; e: −x + 1, y + 1/2, −z + 1)], leading to a three-dimensional supramolecular network (Fig. 1c). In **2**, three types of intrachain hydrogen bonds are formed between two water ligands and carboxylate O atoms [O7—H7F···O1, O7—H7F···O2, O5—H5F···O3a (a: x, y, z + 1)], different from those of **1**. However, the interchain hydrogen bonds [O6—H6E···O4b, O8—H8E···O1c (b: x − 1, y, z + 1; c: x + 1, y, z)] leading to the formation of a 2D-layered network are the same as those of **1** (Fig. 2a). Then the 2D-layered network are connected by four kinds of interlayer hydrogen bonds formed between coordination water molecules with uncoordinated carboxylate O atoms and thiadiazole N atoms [O5—H5E···N2f, O8—H8F···N1f, O6—H6F···O3 g, O7—H7E···O3 g

TABLE III Selected Bond Lengths (Å) and Angles (°) for **1**–**7**

Compound **1**					
Co(1)—O(6)	2.045(3)	Co(1)—O(8)	2.082(3)	Co(1)—O(4)#1	2.094(3)
Co(1)—O(1)	2.116(3)	Co(1)—O(5)	2.127(3)	Co(1)—O(7)	2.156(3)
O(6)—Co(1)—O(8)	177.62(17)	O(6)—Co(1)—O(4)#1	91.65(14)	O(8)—Co(1)—O(4)#1	90.34(15)
O(6)—Co(1)—O(1)	91.26(14)	O(8)—Co(1)—O(1)	86.78(14)	O(4)#1—Co(1)—O(1)	176.83(17)
O(6)—Co(1)—O(5)	89.38(13)	O(8)—Co(1)—O(5)	91.82(13)	O(4)#1—Co(1)—O(5)	92.76(13)
O(1)—Co(1)—O(5)	86.01(13)	O(6)—Co(1)—O(7)	90.93(14)	O(8)—Co(1)—O(7)	87.93(14)
O(4)#1—Co(1)—O(7)	85.66(14)	O(1)—Co(1)—O(7)	95.56(14)	O(5)—Co(1)—O(7)	178.39(14)
Compound **2**					
Ni(1)—O(6)	2.070(3)	Ni(1)—O(8)	2.023(3)	Ni(1)—O(4)#1	2.079(3)
Ni(1)—O(1)	2.059(3)	Ni(1)—O(5)	2.073(3)	Ni(1)—O(7)	2.089(3)
O(6)—Ni(1)—O(8)	179.25(15)	O(6)—Ni(1)—O(4)#1	88.16(14)	O(8)—Ni(1)—O(4)#1	91.10(13)
O(6)—Ni(1)—O(1)	89.14(14)	O(8)—Ni(1)—O(1)	91.59(13)	O(4)#1—Ni(1)—O(1)	176.91(18)
O(6)—Ni(1)—O(5)	88.71(14)	O(8)—Ni(1)—O(5)	91.45(14)	O(4)#1—Ni(1)—O(5)	95.09(13)
O(1)—Ni(1)—O(5)	86.36(13)	O(6)—Ni(1)—O(7)	90.84(13)	O(8)—Ni(1)—O(7)	89.01(13)
O(4)#1—Ni(1)—O(7)	86.18(13)	O(1)—Ni(1)—O(7)	92.35(13)	O(5)—Ni(1)—O(7)	178.64(13)
Compound **3**					
Zn(1)—O(6)	2.083(6)	Zn(1)—O(8)	2.190(6)	Zn(1)—O(4)#1	2.105(6)
Zn(1)—O(1)	2.028(5)	Zn(1)—O(5)	2.147(6)	Zn(1)—O(7)	2.070(7)
O(6)—Zn(1)—O(8)	173.5(3)	O(6)—Zn(1)—O(4)#1	90.1(3)	O(8)—Zn(1)—O(4)#1	84.3(2)
O(6)—Zn(1)—O(1)	94.9(3)	O(8)—Zn(1)—O(1)	90.5(2)	O(4)#1—Zn(1)—O(1)	174.4(3)
O(6)—Zn(1)—O(5)	88.4(3)	O(8)—Zn(1)—O(5)	88.3(2)	O(4)#1—Zn(1)—O(5)	89.4(3)
O(1)—Zn(1)—O(5)	88.2(3)	O(6)—Zn(1)—O(7)	87.3(3)	O(8)—Zn(1)—O(7)	95.5(3)
O(4)#1—Zn(1)—O(7)	86.1(3)	O(1)—Zn(1)—O(7)	96.6(3)	O(5)—Zn(1)—O(7)	173.8(3)
Compound **4**					
Zn(1)—O(2)#1	2.040(2)	Zn(1)—O(1)	2.052(2)	Zn(1)—N(4)#2	2.141(2)
Zn(1)—N(3)	2.143(2)	Zn(1)—O(4)#3	2.144(2)	Zn(1)—O(3)#3	2.389(2)
O(2)#1—Zn(1)—O(1)	121.90(9)	O(2)#1—Zn(1)—N(4)#2	86.43(8)	O(1)—Zn(1)—N(4)#2	90.02(9)
O(2)#1—Zn(1)—N(3)	86.92(8)	O(1)—Zn(1)—N(3)	97.54(8)	N(4)#2—Zn(1)—N(3)	171.83(9)
O(2)#1—Zn(1)—O(4)#3	147.09(9)	O(1)—Zn(1)—O(4)#3	90.99(9)	N(4)#2—Zn(1)—O(4)#3	95.20(8)
N(3)—Zn(1)—O(4)#3	87.81(9)	O(2)#1—Zn(1)—O(3)#3	89.98(8)	O(1)—Zn(1)—O(3)#3	147.48(8)
N(4)#2—Zn(1)—O(3)#3	85.45(9)	N(3)—Zn(1)—O(3)#3	89.79(9)	O(4)#3—Zn(1)—O(3)#3	57.53(8)
Compound **5**					
Cd(1)—O(5)	2.2385(14)	Cd(1)—N(3)	2.3288(15)	Cd(1)—O(4)#1	2.3320(13)
Cd(1)—O(3)#2	2.3347(15)	Cd(1)—O(2)	2.3698(15)	Cd(1)—O(1)	2.4722(13)
O(5)—Cd(1)—N(3)	88.95(6)	O(5)—Cd(1)—O(4)#1	141.03(5)	N(3)—Cd(1)—O(4)#1	87.47(5)
O(5)—Cd(1)—O(3)#2	133.23(5)	N(3)—Cd(1)—O(3)#2	83.30(6)	O(4)#1—Cd(1)—O(3)#2	84.78(4)
O(5)—Cd(1)—O(2)	98.10(7)	N(3)—Cd(1)—O(2)	164.02(6)	O(4)#1—Cd(1)—O(2)	95.77(6)
O(3)#2—Cd(1)—O(2)	81.43(6)	O(5)—Cd(1)—O(1)	81.11(5)	N(3)—Cd(1)—O(1)	141.85(5)
O(4)#1—Cd(1)—O(1)	78.13(5)	O(3)#2—Cd(1)—O(1)	129.34(5)	O(2)—Cd(1)—O(1)	53.92(5)
Compound **6**					
Co(1)—O(1)	2.0847(11)	Co(1)—O(4)#1	2.1024(11)	Co(1)—O(5)	2.1103(12)
Co(1)—O(3)#2	2.1253(11)	Co(1)—N(3)	2.1406(12)	Co(1)—N(4)#3	2.1536(12)
O(1)—Co(1)—O(4)#1	92.58(4)	O(1)—Co(1)—O(5)	85.68(5)	O(4)#1—Co(1)—O(5)	175.28(5)
O(1)—Co(1)—O(3)#2	176.12(4)	O(4)#1—Co(1)—O(3)#2	85.63(4)	O(5)—Co(1)—O(3)#2	96.36(4)
O(1)—Co(1)—N(3)	91.05(4)	O(4)#1—Co(1)—N(3)	90.66(5)	O(5)—Co(1)—N(3)	93.76(5)
O(3)#2—Co(1)—N(3)	85.53(4)	O(1)—Co(1)—N(4)#3	93.84(5)	O(4)#1—Co(1)—N(4)#3	91.55(5)
O(5)—Co(1)—N(4)#3	84.20(5)	O(3)#2—Co(1)—N(4)#3	89.65(4)	N(3)—Co(1)—N(4)#3	174.54(5)
Compound **7**					
Ni(1)—O(1)	2.060(3)	Ni(1)—O(9)	2.074(3)	Ni(1)—O(4)#1	2.085(3)
Ni(1)—N(5)	2.086(3)	Ni(1)—N(8)#2	2.087(3)	Ni(1)—O(3)#3	2.118(3)
Ni(2)—O(10)	2.046(3)	Ni(2)—O(5)	2.071(3)	Ni(2)—O(7)#4	2.078(3)
Ni(2)—N(6)	2.090(3)	Ni(2)—N(7)	2.097(3)	Ni(2)—O(8)#5	2.132(3)
O(1)—Ni(1)—O(9)	88.09(11)	O(1)—Ni(1)—O(4)#1	177.28(10)	O(9)—Ni(1)—O(4)#1	93.46(11)
O(1)—Ni(1)—N(5)	90.63(11)	O(9)—Ni(1)—N(5)	95.92(12)	O(4)#1—Ni(1)—N(5)	86.99(11)
O(1)—Ni(1)—N(8)#2	91.83(11)	O(9)—Ni(1)—N(8)#2	85.92(13)	O(4)#1—Ni(1)—N(8)#2	90.51(11)
N(5)—Ni(1)—N(8)#2	176.98(12)	O(1)—Ni(1)—O(3)#3	93.16(11)	O(9)—Ni(1)—O(3)#3	173.98(12)
O(4)#1—Ni(1)—O(3)#3	85.53(10)	N(5)—Ni(1)—O(3)#3	89.95(12)	N(8)#2—Ni(1)—O(3)#3	88.16(12)
O(10)—Ni(2)—O(5)	86.22(11)	O(10)—Ni(2)—O(7)#4	179.11(11)	O(5)—Ni(2)—O(7)#4	92.94(11)
O(10)—Ni(2)—N(6)	91.27(13)	O(5)—Ni(2)—N(6)	91.98(11)	O(7)#4—Ni(2)—N(6)	89.08(11)
O(10)—Ni(2)—N(7)	90.24(13)	O(5)—Ni(2)—N(7)	92.09(11)	O(7)#4—Ni(2)—N(7)	89.47(11)
N(6)—Ni(2)—N(7)	175.75(12)	O(10)—Ni(2)—O(8)#5	94.64(11)	O(5)—Ni(2)—O(8)#5	176.99(10)
O(7)#4—Ni(2)—O(8)#5	86.18(10)	N(6)—Ni(2)—O(8)#5	90.89(11)	N(7)—Ni(2)—O(8)#5	85.03(11)

Symmetry transformations used to generate equivalent atoms: For **1**: #1 x, y, z + 1; #2 x, y, z − 1. For **2**: #1 x, y, z + 1; #2 x, y, z − 1. For **3**: #1 x, y, z + 1; #2 x, y, z − 1. For **4**: #1: −x, −y, −z + 1; #2: x, y, z + 1; #3: x, y − 1, z + 1; #4: x, y + 1, z − 1; #5: x, y, z − 1. For **5**: #1: x − 1/2, − y + 3/2, z + 1/2; #2: −x + 2, −y + 1, −z; #3: x + 1/2, −y + 3/2, z − 1/2; #4: −x + 1, −y + 1, −z + 1. For **6**: #1: −x, −y, −z + 1; #2: x + 1/2, −y + 1/2, −z + 1; #3: x, −y + 1/2, z − 1/2; #4: x − 1/2, −y + 1/2, −z + 1; #5: x, −y + 1/2, z + 1/2. For **7**: #1; −x + 2, y + 1/2, −z + 1/2; #2: x + 1, y, z; #3: −x + 2, −y, −z; #4: −x + 1, −y, −z + 1; #5: −x + 1, y + 1/2, −z + 1/2; #6: −x + 2, y − 1/2, −z + 1/2; #7: −x + 1, y − 1/2, −z + 1/2; #8: x − 1, y, z.

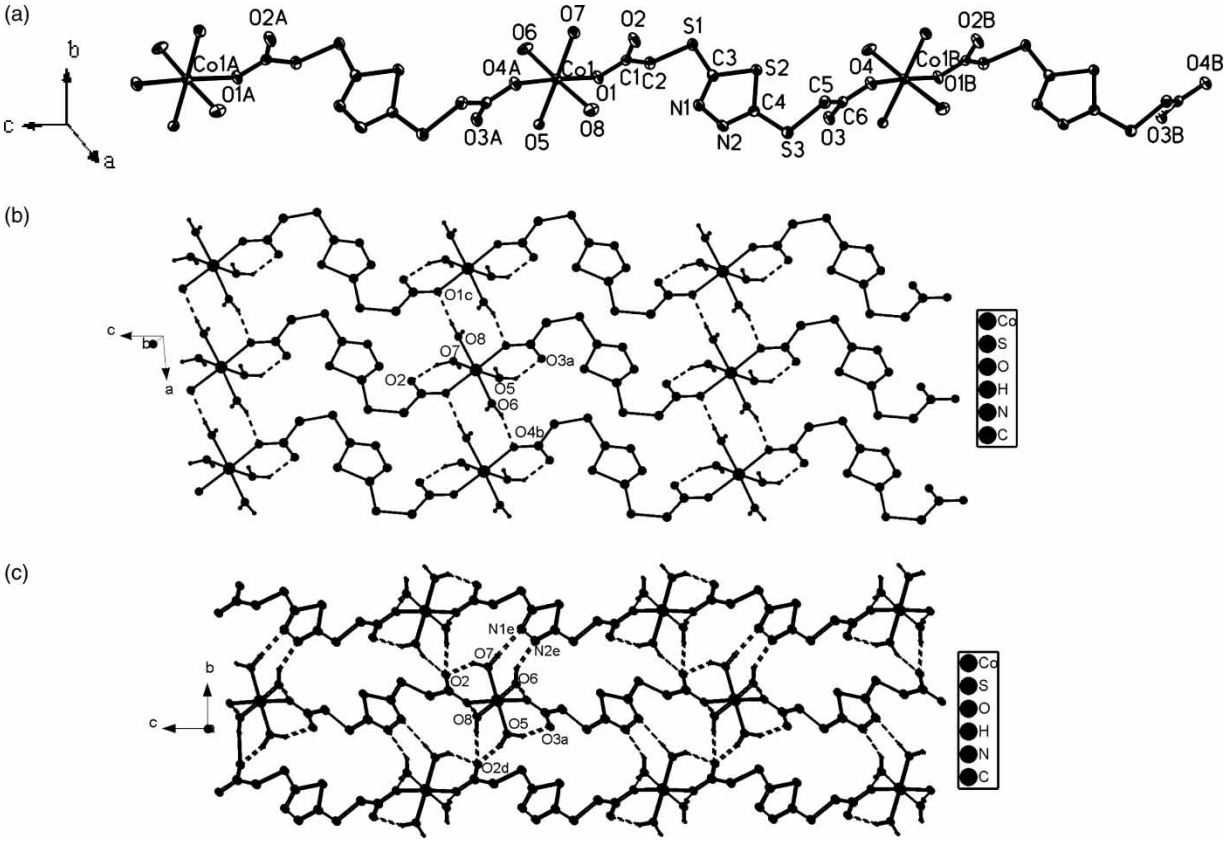

FIGURE 1 (a) One-dimensional chain structure of **1** along the *c* axis, drawn with the ellipsoids at the 30% probability level (hydrogen atoms were omitted for clarity); (b) The 2D-hydrogen-bonding supramolecular layered-structure of **1** in *ac* plane (irrelevant hydrogen atoms are omitted for clarity); (c) The 3D-hydrogen-bonding supramolecular network of **1** viewed along *a* axis.

(f: −x, y − 1/2, −z + 1; g: −x, y + 1/2, −z + 1)] to construct a 3D supramolecular structure (Fig. 2b). Unlike those of **1** and **2**, only one sort of intrachain hydrogen bond exist [O5—H5E···O3a (a: x, y, z + 1)] and three sorts of interchain hydrogen bonds [O6—H6F···O4b, O8—H8E···O5c, O8—H8F···O1c (b: x − 1, y, z + 1; c: x + 1, y, z)] form an infinite 2D-layered network in **3**. Among the layers, except for hydrogen bonds formed between ligated water molecules with uncoordinated carboxylate O atoms [O5—H5F···O2d] or thiadiazole N atoms [O6—H6E···N2e O7—H7E···N1e (e: −x + 1, y + 1/2, −z + 1)], a new sort of hydrogen bonding interaction between water ligands and thiadiazole S atoms [O5—H5E···S1 h (h: −x, y − 1/2, −z + 1)] appears (Fig. 2c). The separations of O···O and O···N in **1**–**3** are in the range of 2.691(5)–3.137(8) Å and 2.776(5)–2.958(6) Å, respectively, while the O···S separation in **3** is 3.367(6) Å, and the bond angles are in the region of 113.3–177.2°, being in the normal range of such non-covalent interactions [38]. In addition, the nonbonding S1···S3 and S2···S3 distances between two adjacent 2D frameworks in **3** are 3.629 Å and 3.484 Å, which are less than the sum of the van der Waals' radii of two S atoms and indicate weak S···S interactions (Fig. 2c) [39–41]. These S···S weak interactions have not been observed in **1** and **2**. Thus the formation of 3D supramolecular networks of **1** and **2** mainly depends on intermolecular hydrogen bonding interactions, whereas the 3D supramolecular network of **3** basically rest on combining the hydrogen-bonding and S···S interactions.

Crystal Structure of [Zn(tzda)(4,4′-bipy)]$_n$ (4)

X-ray diffraction analysis of compound **4** reveals an infinite 2-D coordination polymeric structure built from [Zn(tzda)]$_n$ double chain motif linking 4,4′-bipy spacers. As shown in Fig. 3a, each Zn(II) atom exhibits a highly distorted octahedral coordination environment formed by four O atoms from three different tzda ligands occupying the equatorial plane, and two 4,4′-bipy N atoms occupying the axial sites. The Zn—O bond lengths range from 2.040(2) Å to 2.389(2) Å, while the axial Zn1—N3 and Zn1—N4A bond distances are 2.143(2) Å and 2.144(2) Å, respectively. These Zn—O and Zn—N distances can be compared to those found in several Zn-carboxylate-4,4′-bipy coordination polymers [42–44]. The bond angles around each Zn(II) atom vary from 85.45(9)° to 171.83(9)° and the two pyridyl rings are basically coplanar, only slightly twisted by 8.1°.

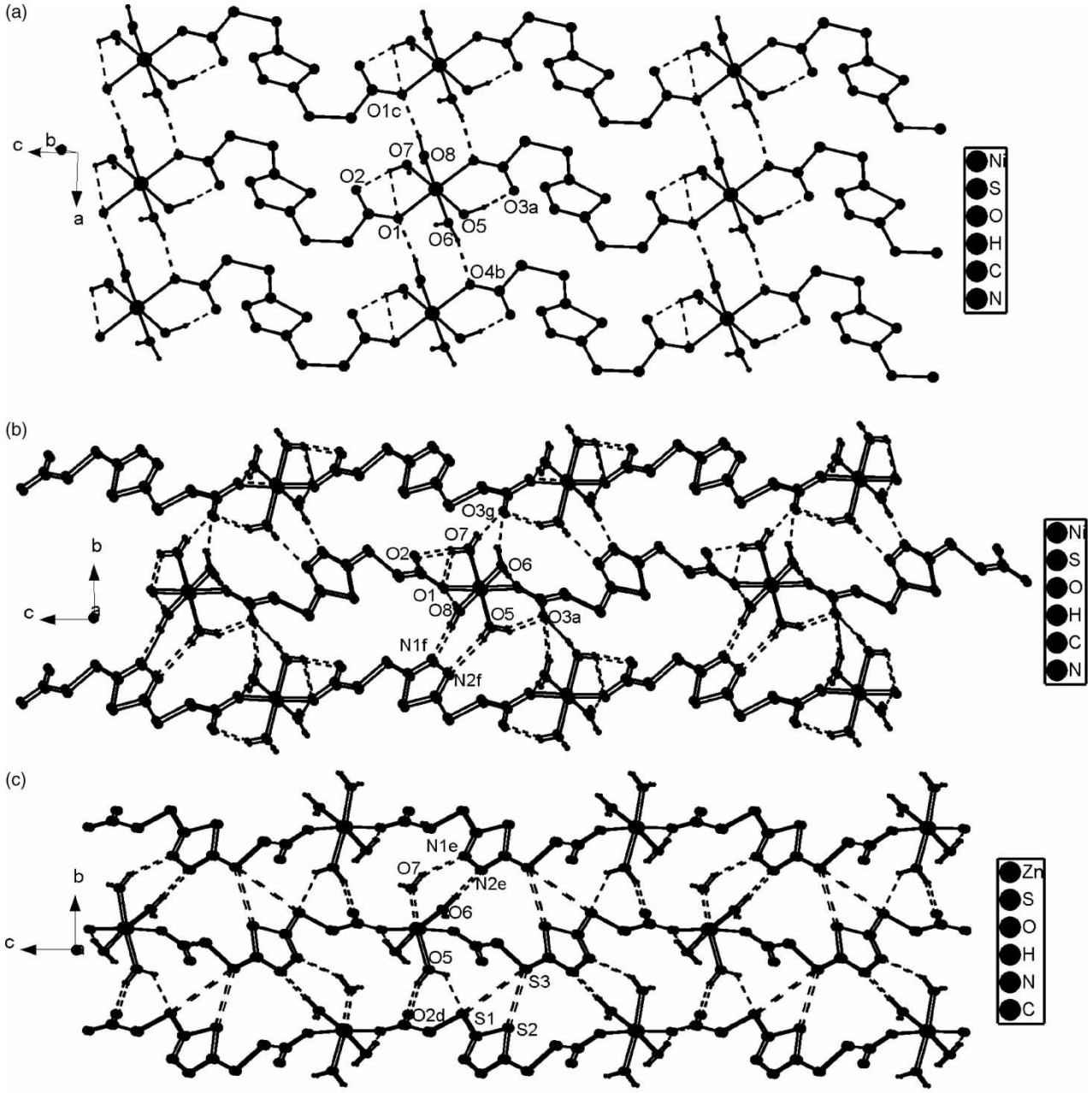

FIGURE 2 (a) The 2D-hydrogen-bonding supramolecular layered-structure of **2** in *ac* plane; (b) The 3D-hydrogen-bonding supramolecular network of **2** viewed along *a* axis; (c) The 3D supramolecular network of **3** viewed along *a* axis, showing the hydrogen-bonding and S···S weak interactions (irrelevant hydrogen atoms are omitted for clarity).

It is noteworthy that, different from that of **1**–**3**, each tzda ligand in **4** adopts *trans*-configuration and acts as a μ_3-bridging ligand to link three Zn atoms through its one chelating carboxylate and one *syn,syn*-bridging carboxylate group. The flexibility of tzda accommodates the formation of 1D $[Zn(tzda)]_n$ zigzag double chain motif running in the direction perpendicular to diagonal between the *b*- and *c*-axes and containing both doubly carboxylate-bridged dizinc units and the 24-membered $[Zn_2(tzda)_2]$ metallocycles (Fig. 3b). The Zn···Zn distances in the dizinc units are 4.069 Å, while the Zn···Zn separation across a tzda ligand is 8.928 Å. These double chains are then crossslinked by 4,4′-bipy into an infinite 2D double-layered network (Fig. 3c) with an interlayer separation of *ca*. 3.784 Å.

Crystal Structure of $[Cd(tzda)(4,4'\text{-bipy})_{0.5}(H_2O)]_n$ (5)

Compound **5** is also an infinite 2D layered network, where every Cd atom is also six-coordinated in a significantly distorted octahedral environment. The equatorial plane is defined by two oxygen atoms [O1, O2] from one chelating carboxylate group, one *syn*-carboxylate oxygen atom [O3A($-x + 2$, $-y + 1$, $-z$)], and one nitrogen atom (N3) from 4,4′-bipy

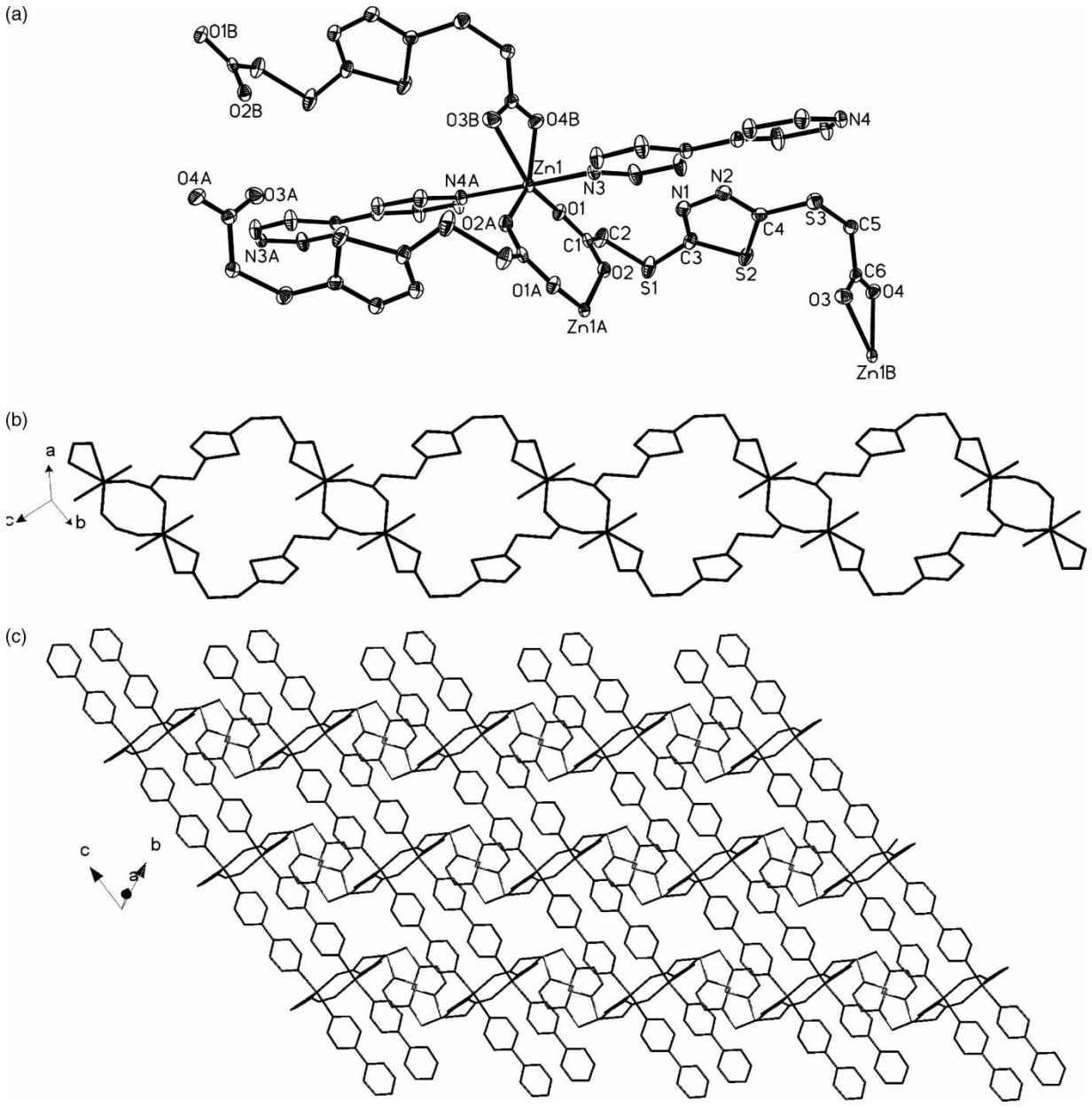

FIGURE 3 (a) Perspective view showing coordination environment of Zn and the bridging mode of tzda with the ellipsoids drawn at the 30% probability level in **4** (hydrogen atoms were omitted); (b) double chain structure composed of Zn atoms and tzda ligands along the direction perpendicular to diagonal between the *b*- and *c*-axes (4,4′-bipy have been omitted); (c) 2D double-layer structure of **4** viewed along *a* axis.

(Fig. 4a). One *anti*-carboxylate oxygen atom and one coordinated water molecule occupy the axial positions of the octahedron with O4B—Cd—O5 bond angle of 141.03(5)°. The Cd—N bond length is 2.3288(15) and the Cd—O bond lengths fall in the range of 2.2385(14)–2.4722(13) Å, which are consistent with reported Cd—N and Cd—O coordination distances [45–47].

Each tzda ligand adopts *trans*-configuration and acts as a μ_3-bridge through one chelating carboxylate group and one *syn,anti*-bridging carboxylate group linking Cd centers. The tzda ligand along with bidentate 4,4′-bipy bridge Cd atoms to construct a 2D layered structure as shown in Fig. 4b. Within this network, the Cd ions are interconnected through *syn,anti*-bridging carboxylate groups, forming a —OCO—Cd—OCO—Cd— chain that extends in the *b* direction. These 1D infinite chains are further linked by a pair of $-CH_2SC_2N_2SSCH_2-$ spacers of tzda anions and 4,4′-bipy spacers alternately along the direction perpendicular to diagonal between the *a*- and *c*-axes, resulting in the formation of the 2D network. The Cd···Cd distances along a pair of μ-tzda ligands and μ-4,4′-bipy are 12.256 Å and 11.766 Å, respectively. The two pyridyl rings in 4,4′-bipy are coplanar, and $\pi-\pi$ stacking interactions exist between the pyridyl ring and the adjacent parallel thiadiazole ring with centroid-to-centroid distance

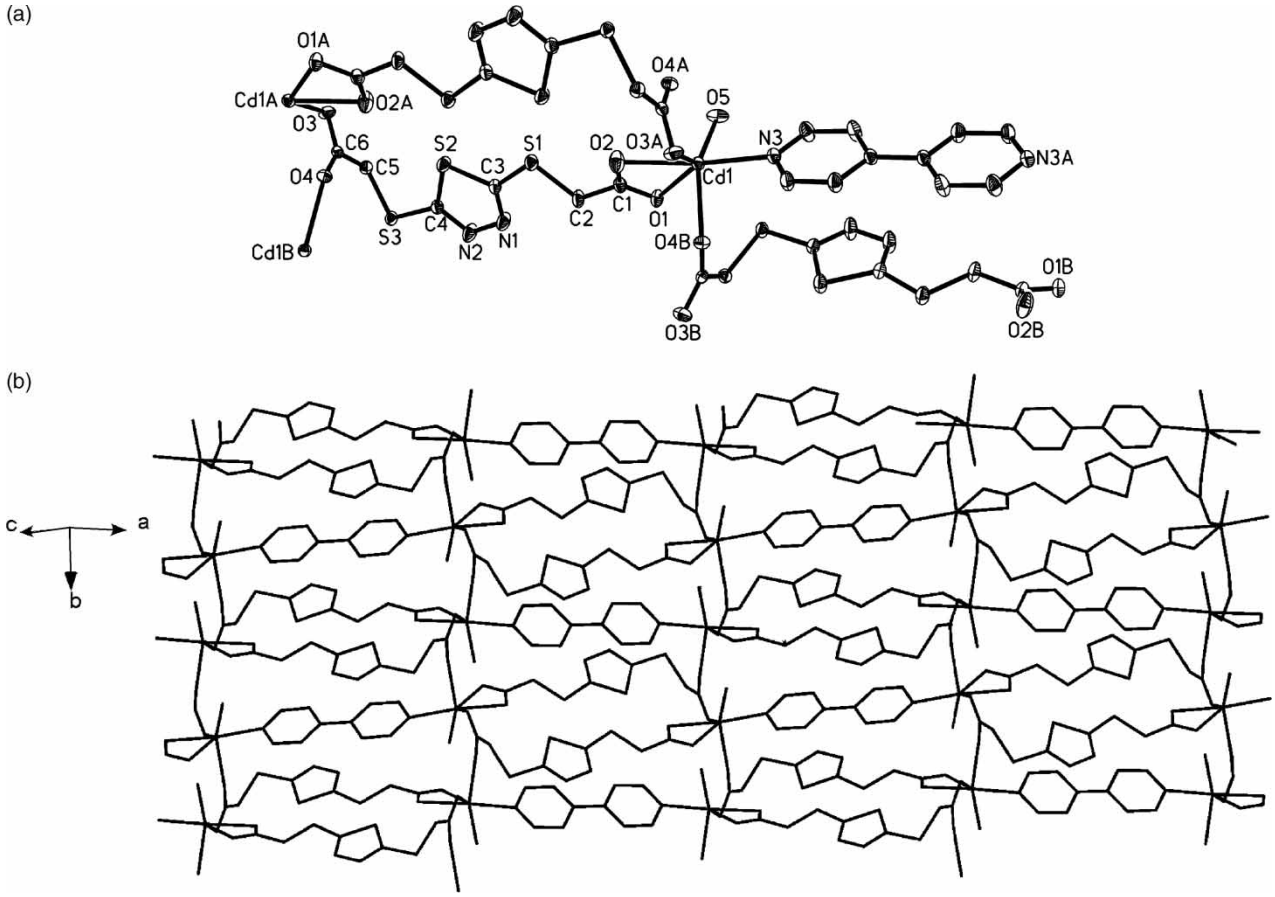

FIGURE 4 (a) Perspective view showing coordination environment of Cd and the bridging mode of tzda with the ellipsoids drawn at the 30% probability level in **5** (hydrogen atoms were omitted); (b) 2D-layered structure of **5** along *b* axis.

of 3.5715 Å. Coordinated water molecules are pointed out and well positioned to form O—H···O hydrogen bonds with carboxylate oxygen atoms (Table SI, Supplementary Material). These hydrogen bonds extend 2D layered network into a 3D supramolecular framework along the diagonal direction of *ac* plane.

Crystal Structure of [Co(tzda)(4,4′-bipy)(H$_2$O)]$_n$ (6)

Compound **6** is an infinite 3D network composed of [Co(tzda)]$_n$ 2D-layered motif linking 4,4′-bipy spacers. As depicted in Fig. 5a, each Co atom coordinates with four oxygen atoms from three individual tzda ligands and one water molecule in the equatorial plane, and two 4,4′-bidy molecules in axial positions. The axial Co1—N3 and Co1—N4 bond distances are 2.1406(12) Å and 2.1536(12) Å, respectively, while Co—O bond distances in equatorial plane are in the range of 2.0847(11)—2.1253(11) Å. The axial N3—Co1—N4A angle is 174.54(5)°, while the equatorial angles, O4B—Co1—O1, O1—Co1—O5, O5—Co1—O3A, and O3A—Co1—O4B are 92.58(4)°, 85.68(5)°, 96.36(4)°, 85.63(4)°, respectively, leading to a slightly distorted octahedral coordination geometry.

Each tzda ligand in **6** still exhibits *trans*-configuration and serves as triconnector (μ_3) linking three metal centers, similar to those in **4** and **5**. Whereas, the bridging mode is obviously different from that in **4** and **5**, the tzda ligand in **6** uses one monodentate carboxylate and the other *syn, anti*-bridging carboxylate group to connect Co atoms. Thus each tzda ligand links three Co atoms and each Co atom coordinates to three tzda ligands to form a 2D-layered framework motif of [Co(tzda)]$_n$ in *ab* plane (Fig. 5b). Within this network, the Co ions are interconnected through *syn, anti*-bridging carboxylate groups, forming a —OCO—Co—OCO—Co— chain that extends along *b* axis; the Co···Co separation relative to the bridging carboxylate group is 5.250 Å. Furthermore, distinctive binuclear 24-membered and tetranuclear 34-membered metallocycles are also observed, which arranged alternately along *a* axis and *b* axis (Fig. 5b). In the 24-membered metallocycle, the Co···Co separation is 10.450 Å, while in the 34-membered metallocycle four Co centers are exactly coplanar and the Co···Co distances bridged by μ-tzda ligand is 11.880 Å.

Interestingly, due to the flexible feature of tzda, the 2D-coordination layer motif presents 'the Great Wall' shape of China viewed along *b* axis (Fig. 5b), which is the most import structural feature of **6** and rarely observed in reported 2D-layered structure. The rigid

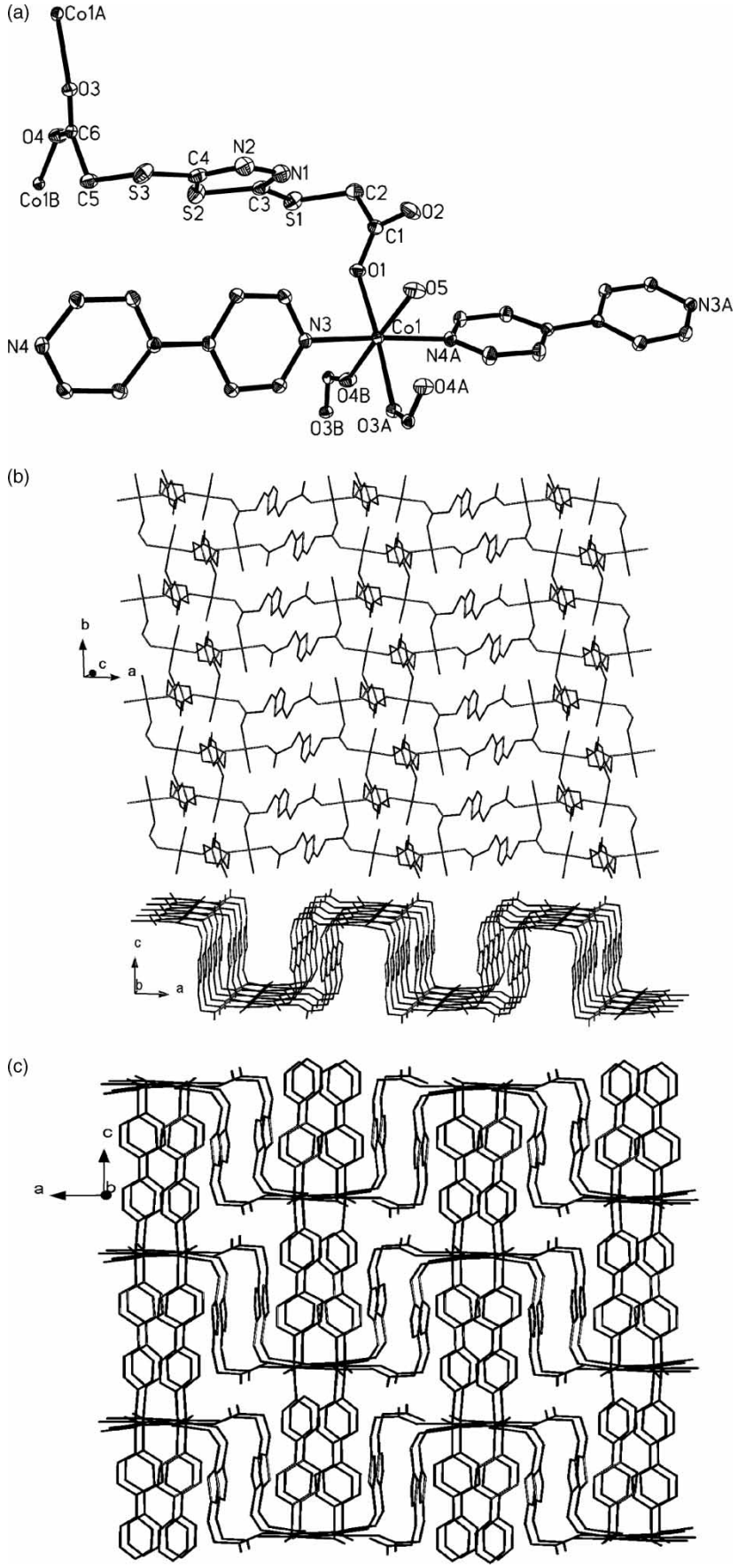

FIGURE 5 (a) Perspective view showing coordination environment of Co and the bridging mode of tzda with the ellipsoids drawn at the 30% probability level in **6** (hydrogen atoms were omitted); (b) 2D-layered architecture constructed by tzda and Co atoms in *ab* plane and viewed along *b* axis, showing the characteristic shape of 'the Great Wall' of China; (c) 3D network of **6** viewed along *b* axis.

4,4′-bipy acts as a pillar linking the adjacent [Co(tzda)$_n$] layers to an extended infinite 3D network (Fig. 5c). Additionally, there exist two types of O—H···O hydrogen bonds and one type of O—H···S hydrogen bond between coordinated water molecules and adjacent tzda ligands in 2D [Co(tzda)]$_n$ layer (Table SI, supplementary material), which further stabilize the three-dimensional architecture of **6**.

Crystal Structure of [Ni(tzda)(4,4′-bipy)(H$_2$O)]$_n$ (7)

Compound **7** features the similar infinite 3D network architecture as **6** does. However, different from **6**, there are two Ni centers in the building unit, as illustrated in Fig. 6a. Ni1 and Ni2 are both coordinated by three oxygen atoms from three tzda ligands, two nitrogen atoms from two 4,4′-bipy, and two water molecules, completing contorted octahedral coordination environment. The Ni1—N and Ni2—N bond lengths are nearly same, being in the range of 2.086(3)—2.097(3) Å. The Ni—O bond distances fall in the range of 2.046(3)—2.132(3) Å and the axial N5—Ni1—N8E (x + 1, y, z) and N6—Ni2—N7 angles are 176.98(12)° and 175.75(12)°, respectively.

It is worth to note that there are two kinds of tzda ligands, which coordinate with Ni1 and Ni2 atoms, respectively, and both display *trans*-configuration. Each tzda ligand acts as μ_3-bridge through one monodentate and one *syn,anti*-bridging carboxylate groups linking three Ni1 or Ni2 atoms. Thus the Ni1 atoms are connected by one kind of tzda ligands to form 2D [Ni1(tzda)]$_n$ layer, and the Ni2 atoms are joined by another kind of tzda ligands to form 2D [Ni2(tzda)]$_n$ layer in *bc* plane. The [Ni1(tzda)]$_n$ and [Ni2(tzda)]$_n$ layers have the similar structural characteristics as that of [Co(tzda)]$_n$ layer in **6**. Namely, the two 2D-coordination layer motifs also

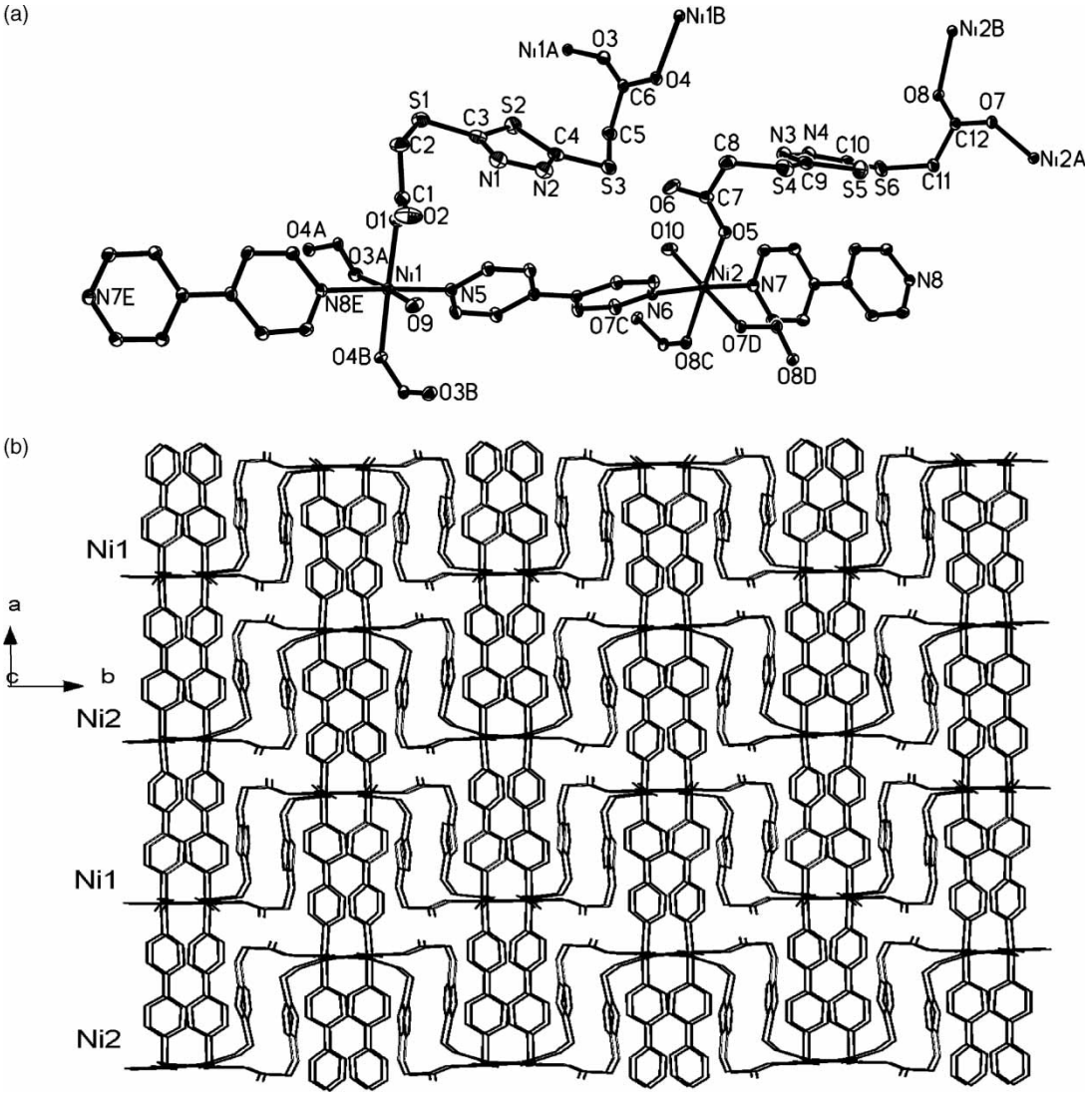

FIGURE 6 (a) Perspective view showing coordination environment of Ni and the bridging mode of tzda with the ellipsoids drawn at the 30% probability level in **7** (hydrogen atoms were omitted); (b) 3D network of **7** viewed along *c* axis.

show the 'the Great Wall' shape of China viewed along *b* axis. Along *a* axis, two kinds of rigid 4,4′-bipy molecules bridge Ni1 and Ni2 atoms to form a linear chain —Ni1—4,4′-bipy(1)—Ni2—4,4′-bipy(2)—Ni1—4,4′-bipy(1)—Ni2—4,4′-bipy(2)—, and through sharing the Ni1 and Ni2 nodes alternately, $[Ni1(tzda)]_n$ layer, $[Ni2(tzda)]_n$ layer and above linear chain construct a 3D network similar to that of **6** (Fig. 6b). Furthermore, coordinated water molecules form interlayer O—H···O hydrogen bonds with carboxylate oxygen atoms of tzda ligands and further stabilize the 3D network of **7** (Table SI, Supplementary Material).

IR Spectra and Thermogravimetric Analysis

The IR spectra of **1**–**7** show the characteristic absorptions of tzda anion. The disappearance of the band at about 1710–1740 cm^{-1} in **1**–**7** assigned to the stretching bands of —COOH indicates complete deprotonation of the carboxyl groups. The strong bands at 1602, 1387 cm^{-1} for **1**, 1599, 1388 cm^{-1} for **2**, 1601, 1392 cm^{-1} for **3**, 1603, 1589 and 1413, 1393 cm^{-1} for **4**, 1582 and 1412, 1389 cm^{-1} for **5**, 1608, 1577 and 1403, 1381 cm^{-1} for **6**, and 1609, 1570 and 1407, 1383 cm^{-1} for **7** are assigned to the asymmetric and symmetric stretching bands of COO^- groups, respectively, suggesting that the COO^- groups functions in different coordination modes [48]. Compounds **1**–**3** and **5**–**7** also show broad —OH stretching bands in the region of 3247–3507 cm^{-1}, indicating the presence of water molecules in these compounds. The analyses of IR spectra of **1**–**7** are in good agreement with crystal structures and charge balance considerations.

Compounds **1**–**7** are stable at ambient conditions, and thermogravimetric experiments were carried out to explore their thermal stabilities (Fig. S1, Supplementary Material). The TGA curves of **1 3** are similar and all exhibit two main steps of weight losses. The first weight loss of 17.96% happens between 104°C and 165°C for **1**, 17.68% between 118°C and 174°C for **2**, 17.57% between 97°C and 167°C for **3**, respectively, which can be attributed to the loss of four coordinated water molecules (calculated: 18.21% for **1**, 18.22% for **2**, and 17.92% for **3**). The second loss occurs at a temperature above 254°C for **1**, above 258°C for **3**, and above 245°C for **3**, respectively, which can be caused by the decomposition of the tzda ligands, and do not end until 950°C. For **4**, the TGA measurement indicates that the 2D framework remains stable upon heating until a continuous weight losses starting from 269°C and not ending until 800°C. Compounds **5**–**7** also have similar TGA curves, the initial weight loss of 3.52% from 164°C to 219°C for **5**, 3.28% from 158°C to 194°C for **6**, and 3.12% from 191°C to 223°C for **7**, respectively, corresponding to the removal of one coordinated water molecule (calculated: 3.81% for **5**, 3.62% for **6**, and 3.62% for **7**), and then another weight loss after the temperature 259°C for **5**, 289°C for **6** and 293°C for **7** begins, which may be assigned to the decomposition of the organic moieties.

Photoluminescent Properties

Metal-organic polymers with d^{10} configuration have been found to exhibit photoluminescence properties and have potential applications in optoelectronic devices and as fluorescent sensors [49–53]. The luminescent properties of free ligand H_2tzda and compounds **3**–**5** are investigated in the solid state at room temperature. As it can be seen from Fig. 7, the ligand H_2tzda displays an emission band at 375 nm upon photoexcitation at 315 nm, which can be attributable to the $\pi^* \rightarrow \pi$ transition; and **3**–**5** exhibit intense emission peaks at 381 nm ($\lambda_{ex} = 324$ nm, for **3**), 454 nm ($\lambda_{ex} = 355$ nm, for **4**), and 447 nm ($\lambda_{ex} = 357$ nm, for **5**), respectively. Therefore, the emission band at 381 nm for **3**, which is only red-shift of 6 nm with respect to H_2tzda ligand, may also attribute to the intraligand transition. While the emission bands at 454 nm for **4** and 447 nm for **5** are obviously different to that of H_2tzda ligand, and accordingly may be assigned to ligand-to-metal charge transfer (LMCT) [54–57]. Furthermore, compared with **4**, a blue-shift of emission occurs for **5**, which is probably due to the differences of central metal ions and coordination environment around them, because photoluminescence behavior is closely associated with the metal ions and the ligands coordinated around them [58]. The results suggest that both **4** and **5** may be prospective candidates for potential luminescent materials [59,60].

Magnetic Properties

The magnetic susceptibility measurements of compounds **6** and **7** were carried out in the 5–300 K temperature range. The magnetic behavior of **6** is illustrated in Fig. 8 by means of a plot of $\chi_M T$ versus the temperature. The value of $\chi_M T$ at 300 K is equal to 3.45 $cm^3\,mol^{-1}\,K$, which is greater than that expected for the spin-only one for a high-spin Co(II) ion (1.88 $cm^3\,mol^{-1}\,K$). However, this feature is normal in Co(II) complexes, where the $\chi_M T$ value at room temperature is normally larger than expected for isolated ions, indicating that an important orbital contribution is involved [61]. As the temperature is lowered, the value of $\chi_M T$ continuously decreases, reaching a minimum value of 1.71 $cm^3\,mol^{-1}\,K$ at 5 K. Since the 3D structure of compound **6** is constructed by long 4,4′-bipy and —$CH_2SC_2N_2$-$SSCH_2$— spacers bridging 1D —OCO—Co—OCO—Co— chains, thus **6** can be assumed to be 1D complex

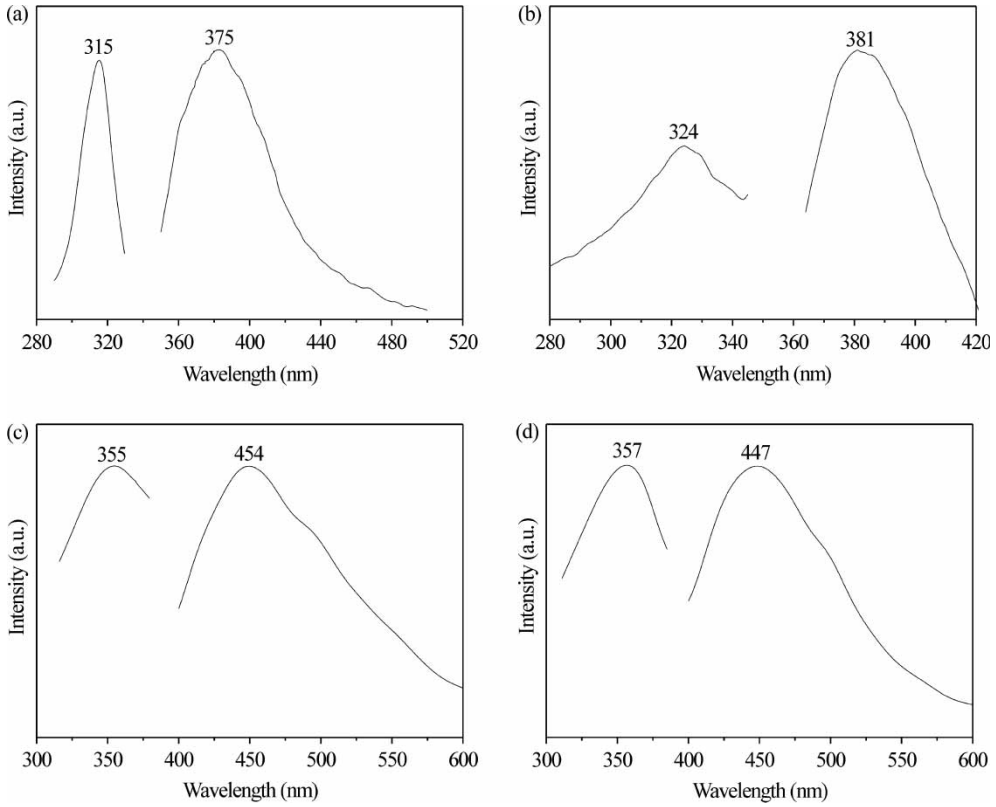

FIGURE 7 Solid-state excitation-emission spectra of compounds at room temperature: (a) H_2tzda; (b) **3**; (c) **4**; (d) **5**.

from magnetic point of view. And for the same 1D —OCO—Co—OCO—Co— chain, Ghosh [61] used the exact solutions of the uniform Ising S = 1/2 chain expanded by Fisher [62] and Katsura [63] (Eqs. (1) and (2)) to simulate the magnetic susceptibility data only at very low temperature, because the degeneracy of $^4T_{1g}$ ground state of the octahedral Co(II) ion prevents an exact fit of the data to any scheme, especially over the entire temperature range, and while in the low temperature range the combination of crystal field distortion and spin-orbit coupling effects slits the $^4T_{1g}$ ground state into six Kramers doublets and causes a spin doublet ground state (S = 1/2) [33].

$$\chi_{\parallel} = Ng^2\beta^2/4kT\exp(2x) \tag{1}$$

$$\chi_{\perp} = Ng^2\beta^2/8kT(|x|^{-1}\tanh|x| + \mathrm{sech}^2 x) \text{ with } x = J/4kT \tag{2}$$

By using the same solutions the magnetic susceptibility data were fitted at the temperature range of $5 - 20\,\mathrm{K}$ and the best-fit parameters are $J = -1.33\,\mathrm{cm}^{-1}$, $g = 4.69$, and $R = 2.1 \times 10^{-4}$ (R is the agreement

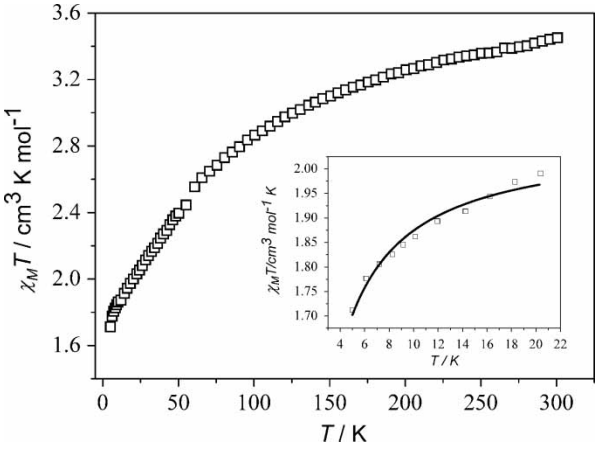

FIGURE 8 Plot of the $\chi_M T$ vs T for compound **6**. Inset: fit of the low-temperature region by the formula given in the text. Solid line represents the best fit with the parameters given in the text.

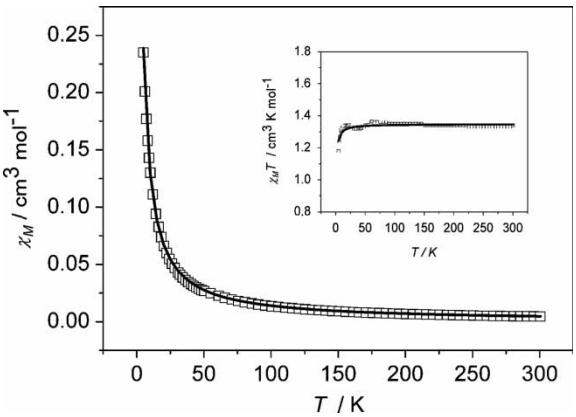

FIGURE 9 Plot of the χ_M and $\chi_M T$ vs T for compound **7**. Solid line represents the best-parameters given in the text.

factor defined as $\Sigma[(\chi_M)_{exp} - (\chi_M)_{cacl}]^2/\Sigma[(\chi_M)_{exp}]^2$ (Fig. 8, inset). The calculated J value indicates an antiferromagnetic interactions between Co(II) ions through carboxylato bridge and may be affected by the spin-orbit coupling.

The χ_M versus T plot and $\chi_M T$ versus T plot for **7** are shown in Fig. 9. At room temperature, the value of χ_M is $0.00444\,cm^3\,mol^{-1}$ ($\chi_M T = 1.34\,cm^3\,mol^{-1}\,K$, typical value for an isolated Ni(II) ion). Upon cooling, χ_M increases gradually to $0.235\,cm^3\,mol^{-1}$ at 5 K. The general features of two curves (χ_M and $\chi_M T$) are characteristic of weak intramolecular antiferromagnetic coupling between nickel ions, which has been observed in the reported compound [Ni(pdc)(4,4′-bipy)]·1/2MeOH(H_2pdc = pyridine-2,6-dicarboxylic acid) [61]. Since **7** has the similar structure as that of **6**, **7** also can be considered as quasi-isolated 1D system from magnetic point of view. An reported empirical formula for analyzing 1D Ni (II) systems is used to fit magnetic susceptibility data [33,61,64].

$$\chi_M = Ng^2\beta^2/kTA/B \quad A = 2.0 + 0.0194x + 0.777x^2$$

$$B = 3.0 + 4.346x + 3.232x^2 + 5.834x^3$$

$$\text{with } x = |J|/kT$$

Using this method, the best-fit parameters for **7** are $J = -0.4\,cm^{-1}$, $g = 2.37$, and $R = 8.7 \times 10^{-7}$ (R is the agreement factor). From the structural point of view, it can be found the Ni(II) ions in **7** are joined through carboxylato groups in *syn-anti* conformation and as a Ni—O—C—O—Ni skeleton is planar, small overlap between the magnetic orbits of nickel ions through the *syn-anti* carboxylato bridge occurs and accounts for the weak antiferromagnetic coupling.

CONCLUSIONS

In summary, seven new metal-organic polymers, $[M(tzda)(H_2O)_4]_n$ [M = Co(**1**), Ni(**2**), Zn(**3**)], $[Zn(tzda)(4,4'\text{-bipy})]_n$ (**4**), $[Cd(tzda)(4,4'\text{-bipy})_{0.5}(H_2O)]_n$ (**5**), $[Co(tzda)(4,4'\text{-bipy})(H_2O)]_n$ (**6**), and $[Ni(tzda)(4,4'\text{-bipy})(H_2O)]_n$ (**7**) were synthesized by hydrothermal methods. Polymers **1**–**3** exhibit similar 1D zigzag chain structures while **4**–**7** display 2D or 3D architectures. As expected, the applying of bridging ligand 4,4′-bipy can help to assembly high-dimensional network in the syntheses of coordination polymers, which indicates the structures of complexes can be manipulated by introducing the secondary ligands. Furthermore, compared with **3**, polymers **4** and **5** incorporating 4,4′-bipy may be potential candidates for blue-light-emitting materials, suggesting the secondary ligands may also effect on the photoluminescent properties of complexes. The magnetic studies in the range 5–300 K indicate that **6** and **7** both display the characteristics of a weak antiferromagnetic coupling between metal ions in the system mediated by carboxylate bridges. This work provides crystal engineering with a potential tool for tuning the crystalline solid architecture and exploring desirable properties.

Acknowledgements

This work was sponsored by the National Natural Science Foundation of China (No. 90610001, 20471053), the China National Key Basic Research Special Funds (No. 2005CB214501, 2006CB708407) and the Energy & Technology Program from Zhengzhou University.

References

[1] Robson, R. *J. Chem. Soc., Dalton Trans.* **2000**, 3735.
[2] Carlucci, L.; Ciani, G.; Proserpio, D. M. *Coord. Chem. Rev.* **2003**, *246*, 247.
[3] Yaghi, O. M.; O'Keeffe, M.; Ockwig, N. W.; Chae, H. K.; Eddaoudi, M.; Kim, J. *Nature* **2003**, *423*, 705.
[4] Kitagawa, S.; Kitaura, R.; Noro, S. *Angew. Chem., Int. Ed.* **2004**, *43*, 2334.
[5] Moulton, B.; Zaworotko, M. J. *Chem. Rev.* **2001**, *101*, 1629.
[6] Davis, M. E. *Nature* **2002**, *417*, 813.
[7] Carlucci, L.; Ciani, G.; Proserpio, D. M.; Porta, F. *Angew. Chem., Int. Ed.* **2003**, *42*, 317.
[8] Rowsell, J. L. C.; Millward, A. R.; Park, K. S.; Yaghi, O. M. *J. Am. Chem. Soc.* **2004**, *126*, 5666.
[9] Rao, C. N. R.; Natarajan, S.; Vaidhyanathan, R. *Angew. Chem. Int. Ed.* **2004**, *43*, 1466.
[10] Mukherjee, P. S.; Konar, S.; Zangrando, E.; Mallah, T.; Ribas, J.; Chaudhuri, N. R. *Inorg. Chem.* **2003**, *42*, 2695.
[11] Millange, F.; Serre, C.; Ferey, G. *Chem. Commun.* **2002**, 822.
[12] Serre, C.; Millange, F.; Thouvenot, C.; Nogues, M.; Marsolier, G.; Louer, D.; Férey, G. *J. Am. Chem. Soc.* **2002**, *124*, 13519.
[13] Rosi, N. L.; Eckert, J.; Eddaoudi, M.; Vodak, D. T.; Kim, J.; O'Keeffe, M.; Yaghi, O. M. *Science* **2003**, *300*, 1127.
[14] Eddaoudi, M.; Kim, J.; Rosi, N.; Vodak, D.; Wachter, J.; O'Keefe, M.; Yaghi, O. M. *Science* **2002**, *295*, 469.
[15] Eddaoudi, M.; Kim, J.; Vodak, D.; Sudik, A.; Wachter, J.; O'Keeffe, M.; Yaghi, O. M. *Proc. Natl. Acad. Sci. U.S.A.* **2002**, *99*, 4900.
[16] Rosi, N. L.; Eddaoudi, M.; Kim, J.; O'Keeffe, M.; Yaghi, O. M. *Angew. Chem., Int. Ed.* **2002**, *41*, 284.
[17] Wang, Y. B.; Zhuang, W. J.; Jin, L. P.; Lu, S. Z. *J. Mol. Struct.* **2004**, *705*, 21.
[18] Liu, Y. H.; Lu, Y. L.; Wu, H. C.; Wang, J. C.; Lu, K. L. *Inorg. Chem.* **2002**, *41*, 2592.
[19] Narinho, M. V.; Yoshida, M. I.; Guedes, K. J.; Krambrock, K.; Bortoluzzi, A. J.; Hörner, M.; Machado, F. C.; Teles, W. M. *Inorg. Chem.* **2004**, *43*, 1539.
[20] Zhang, X.; Guo, G. C.; Zheng, F. K.; Zhou, G. W.; Mao, J. G.; Dong, Z. C.; Huang, J. S.; Mak, T. C. W. *J. Chem. Soc., Dalton Trans.* **2002**, 1344.
[21] Wu, G.; Wang, X. F.; Okama, T.; Sun, W. Y.; Ueyama, N. *Inorg. Chem.* **2006**, *45*, 8543.
[22] Férey, G. *Chem. Mater.* **2001**, *13*, 3084.
[23] Rather, B.; Zaworotko, M. J. *Chem. Commun.* **2003**, 830.
[24] Pan, L.; Adams, K. M.; Hernandez, H. E.; Wang, X.; Zheng, C.; Hattori, Y.; Kaneko, K. *J. Am. Chem. Soc.* **2003**, *125*, 3062.
[25] Hong, X. L.; Bai, J. F.; Song, Y.; Li, Y. Z.; Pan, Y. *Eur. J. Inorg. Chem.* **2006**, 3659.
[26] Zhang, X. F.; Gao, S.; Huo, L. H.; Gao, J. S. *Acta Cryst.* **2006**, *E62*, m39.

[27] Gao, S.; Hou, L. H.; Zhao, H.; Ng, S. W. *Acta Cryst.* **2005**, *E61*, m126.
[28] Lou, X. H.; Zhu, Y.; Gao, H.; Zhu, A. X.; Fan, Y. T.; Hou, H. W.; Lu, H. J. *Wuji Huaxue Xuebao (Chinese)* **2005**, *21*, 716.
[29] Wang, Y. T.; Zhang, L. P.; Fan, Y. T.; Hou, H. W.; Shen, X. Q. *Inorg. Chim. Acta.* **2007**, *360*, 2958.
[30] Lo, S. M. L.; Chui, S. S. Y.; Shek, L. Y.; Lin, Z. Y.; Zhang, X. X.; Wen, G. H.; Williams, I. D. *J. Am. Chem. Soc.* **2000**, *122*, 6293.
[31] Shi, Z.; Feng, S. H.; Sun, Y.; Hua, J. *Inorg. Chem.* **2001**, *40*, 5312.
[32] Tao, J.; Tong, M. L.; Chen, X. M. *J. Chem. Soc., Dalton Trans.* **2000**, 3669.
[33] Kahn, O. *Molecular Magnetism*; VCH publisher: New York, 1993.
[34] Sheldrick, G. M. *SHELXL-97, Program for the Solution and Refinement of Crystal Structures*; University of Göttingen: Germany, 1997.
[35] Rabenau, A. *Angew. Chem., Int. Ed. Engl.* **1985**, *24*, 1026.
[36] Lu, J. Y.; Lawandy, M. L.; Li, J.; Yuen, T.; Lin, C. L. *Inorg. Chem.* **1999**, *38*, 2695.
[37] Wang, R. H.; Zhou, Y. F.; Sun, Y. Q.; Yuan, D. Q.; Han, L.; Lou, B. Y.; Wu, B. L.; Hong, M. C. *Cryst. Growth Des.* **2005**, *5*, 251.
[38] Desiraju, G. R.; Steiner, T. *The Weak Hydrogen Bond in Structural Chemistry and Biology*; Oxford University Press: Oxford, 1999.
[39] De Groot, B.; Jenkins, H. A.; Loeb, S. J. *Inorg. Chem.* **1992**, *31*, 203.
[40] Alberto, R.; Nef, W.; Smith, A.; Kaden, T. A.; Neuburger, M.; Zehnder, M.; Frey, A.; Abram, U.; Schubiger, P. A. *Inorg. Chem.* **1996**, *35*, 3420.
[41] Munakata, M.; Kuroda-Sowa, T.; Maekawa, M.; Hirota, A.; Kitagawa, S. *Inorg. Chem.* **1995**, *34*, 2705.
[42] Wang, M. S.; Guo, G. C.; Cai, L. Z.; Chen, W. T.; Liu, B.; Wu, A. Q.; Huang, J. S. *J. Chem. Soc., Dalton Trans.* **2004**, 2230.
[43] Wen, L. L.; Dang, D. B.; Duan, C. Y.; Li, Y. Z.; Tian, Z. F.; Meng, Q. J. *Inorg. Chem.* **2005**, *44*, 7161.
[44] Li, G.; Hou, H. W.; Li, L. K.; Meng, X. R.; Fan, Y. T.; Zhu, Y. *Inorg. Chem.* **2003**, *42*, 4995.
[45] Li, X. J.; Cao, R.; Bi, W. H.; Wang, Y. Q.; Wang, Y. L.; Li, X.; Guo, Z. G. *Cryst. Growth Des.* **2005**, *5*, 1651.
[46] Shi, X.; Zhu, G. S.; Wang, X. H.; Li, G. H.; Fang, Q. R.; Wu, G.; Tian, G.; Xue, M.; Zhao, X. J.; Wang, R. W.; Qiu, S. L. *Cryst. Growth Des.* **2005**, *5*, 207.
[47] Li, F.; Ma, Z.; Wang, Y. L.; Cao, R.; Bi, W. H.; Li, X. *Cryst. Eng. Comm.* **2005**, *7*, 569.
[48] Deacon, G. B.; Phillips, R. J. *Coord. Chem. Rev.* **1980**, *33*, 227.
[49] Sun, D. F.; Cao, R.; Weng, J. B.; Hong, M. C.; Liang, Y. C. *J. Chem. Soc., Dalton Trans.* **2002**, 291.
[50] Lin, P.; Henderson, R. A.; Harrington, R. W.; Clegg, W.; Wu, C. D.; Wu, X. T. *Inorg. Chem.* **2004**, *43*, 181.
[51] Han, L.; Yuan, D. Q.; Wu, B. L.; Liu, C. P.; Hong, M. C. *Inorg. Chim. Acta.* **2006**, *359*, 2232.
[52] Han, L.; Hong, M.; Wang, R.; Wu, B.; Xu, Y.; Lou, B.; Lin, Z. *Chem. Commun.* **2004**, 2578.
[53] Zhang, J.; Xie, Y. R.; Ye, Q.; Xiong, R. G.; Xue, Z.; You, X. Z. *Eur. J. Inorg. Chem.* **2003**, 2572.
[54] Tao, J.; Shi, J. X.; Tong, M. L.; Zhang, X. X.; Chen, X. M. *Inorg. Chem.* **2001**, *40*, 6328.
[55] Wang, X. L.; Qin, C.; Wang, E. B.; Li, Y. G.; Hao, N.; Hu, C. W.; Xu, L. *Inorg. Chem.* **2004**, *43*, 1850.
[56] Wang, Z.; Zhang, H. H.; Chen, Y. P.; Huang, C. C.; Sun, R. Q.; Cao, Y. N.; Yu, X. H. *J. Solid State Chem.* **2006**, *179*, 1536.
[57] Dai, J. C.; Wu, X. T.; Fu, Z. Y.; Cui, C. P.; Wu, S. M.; Du, W. X.; Wu, L. M.; Zhang, H. H.; Sun, Q. Q. *Inorg. Chem.* **2002**, *41*, 1391.
[58] Fu, Z. Y.; Wu, X. T.; Dai, J. C.; Hu, S. M.; Du, W. X.; Zhang, H. H.; Sun, R. Q. *Eur. J. Inorg. Chem.* **2002**, 2730.
[59] Hassan, A.; Wang, S. *Chem. Commun.* **1998**, 211.
[60] Li, Y. X.; Li, Y. H.; Zeng, X. R.; Xiong, R. G.; You, X. Z.; Fun, H. K. *Inorg. Chem. Commun.* **2003**, *6*, 1144.
[61] Ghosh, S. K.; Ribas, J.; Bharadwaj, P. K. *Cryst. Growth Des.* **2005**, *5*, 623.
[62] Fisher, M. E. *J. Math. Phys. (N.Y.)* **1963**, *4*, 124.
[63] Katsura, S. *Phys. Rev.* **1962**, *127*, 1508.
[64] Weng, C. Y. Ph.D. Thesis; Carnegie Mellon University: Pittsburgh, 1968.